Quantum behavior of a flux qubit coupled to a resonator

A.N. Omelyanchouk[1], S.N. Shevchenko[1,2], Ya.S. Greenberg[3,2], O. Astafiev[4], and E. Il'ichev[2]

[1]*B. Verkin Institute for Low Temperature Physics and Engineering of the National Academy of Sciences of Ukraine*
47 Lenin Ave., 61103 Kharkov, Ukraine
E-mail: sshevchenko@ilt.kharkov.ua

[2]*Institute of Photonic Technology, P.O. Box 100239, D-07702 Jena, Germany*

[3]*Novosibirsk State Technical University, 20 Karl Marx Ave., Novosibirsk, 630092, Russia*

[4]*NEC Nano Electronics Research Laboratories, Tsukuba, Ibaraki, 305-8501, Japan*

The detailed theory for the system of a superconducting qubit coupled to the transmission line resonator is presented. We describe the system by solving analytically and numerically the master equation for the density matrix, which includes dissipative Lindblad term. We calculate the transmission coefficient, which provides the way to probe the dressed states of the qubit. The theoretical results are related to the experiment with the intermediate coupling between the qubit and the resonator, when the coupling energy is of the same order as the qubit relaxation rate.

1. Introduction

The present level of nanotechnology brings together the quantum optics and mesoscopic solid state physics. The systems currently under extensive investigations are the superconducting circuits based on Josephson junctions (Josephson qubits) which are the macroscopic quantum objects, quantum behaviors of which have been demonstrated in experiments (for review see, e.g., Refs. 1–4). Superconducting qubits being quantum mesoscopic objects present possibility to realize several unique quantum phenomena, such as entanglement [5,6], Rabi oscillations [7–12], spin echo and Ramsey fringes [13,14], Landau–Zener–Stückelberg interferometry [15–19], etc. Presently large interest brings over to the problem of the behavior of such artificial atoms in a quantized electromagnetic field in the frame of so-called circuit quantum electrodynamics (CQED) [20]. In CQED a superconducting qubit acting as an artificial atom is electrostatically coupled to a high-quality transmission line resonator. The large effective dipole moment of the qubit and high-energy density of the resonator allowed this system to reach the strong coupling limit of CQED in a solid-state system. This idea was proposed recently and studied theoretically [21–25] and experimentally for the

charge qubit coupled capacitively to the resonator [26–28]. Then inductive coupling for the flux qubit was proposed [29] and realized [30,31].

In this paper we consider the quantum state of the complex system of a superconducting flux qubit coupled to the transmission line resonator. Our aim is firstly to present the detailed theory of the qubit's states, dressed by the interaction with the quantum resonator, and their influence on the observable transmittance. And secondly we aim to describe the regime of intermediate coupling studied recently experimentally by Oelsner et al. [31]. Accordingly, the paper is organized as following. In the next Section the model of the system is presented. In Sec. 3 we calculate the energy levels of the system, matching of which with the driving photons allows for the system's spectroscopy. The Hamiltonian of the driven system is rewritten in Sec. 4 in different representations, in particular, in the rotating-wave approximation (RWA) which is convenient for finding the stationary solutions. The solution of the master equation is presented in Sec. 5 analytically for weak driving and numerically for strong driving. At the end of the paper there are Conclusions and Appendix, in which we present details of the theory of the transmittance through the resonator.

2. Description of the system

We consider the flux qubit coupled inductively to the quantum resonator, see Fig. 1. The flux qubit is the superconducting loop with three Josephson junctions [32]. The basic states of the qubit correspond to different directions of the current in the loop. The current state of the qubit influences the quantum state of the resonator. The quantum resonator we consider to be formed between two interruptions in the transmission line. The qubit is situated close to the center of the resonator; note that the qubit dimensions are significantly smaller than the resonator wavelength, so we can safely ignore its size.

Total Hamiltonian of the driven system, without taking into account relaxation processes, has the form

$$H = H_{qb-r} + H_{\mu w},\qquad(1)$$

where the qubit-resonator Hamiltonian

$$H_{qb-r} = H_{qb} + H_r + H_{int}\qquad(2)$$

consists of the bare qubit and resonator terms and the interaction term. The flux qubit Hamiltonian in the flux basis $\{|\downarrow\rangle, |\uparrow\rangle\}$ has the form [32]

$$H_{qb} = -\frac{\Delta}{2}\tau_x - \frac{\varepsilon}{2}\tau_z,\qquad(3)$$

where Δ is the tunnelling amplitude, the energy bias $\varepsilon = 2I_p(\Phi - \Phi_0/2)$ is defined by the magnetic flux Φ, I_p is the persistent current, $\tau_{x,z}$ are Pauli matrices in the flux basis ($\tau_z|\downarrow\rangle = -|\downarrow\rangle$); the current operator is $I_{qb} = -I_p\tau_z$.

The qubit is considered to be coupled to the transmission line resonator. The detailed theory is presented in the Appendix (see also Refs. 31, 33, 34). The one-mode resonator is described by the following Hamiltonian:

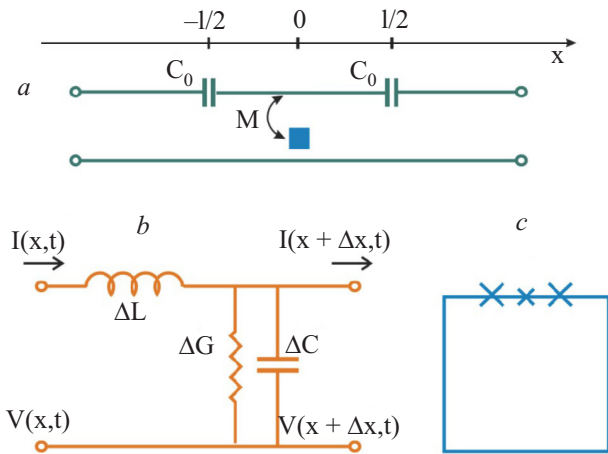$$H_r = \hbar\omega_r\left(a^\dagger a + \frac{1}{2}\right),\qquad(4)$$

Fig. 1. (Color online) (*a*) Scheme of the qubit (denoted by blue box) coupled to the transmission line resonator. (*b*) Equivalent circuit for the description of the infinitesimal piece of length Δx of the transmission line. (*c*) Flux qubit with 3 Josephson junctions.

where a and $a^\dagger$ are the annihilation and creation operators, which act at the number (Fock) states as following: $a|n\rangle = \sqrt{n}|n-1\rangle$ and $a^\dagger|n-1\rangle = \sqrt{n}|n\rangle$.

The term, which describes the interaction of the resonator and the flux qubit, is

$$H_{int} = MI(0)I_{qb} = -\hbar g(a^\dagger + a)\tau_z,\qquad(5)$$

$$\hbar g = MI_{r0}I_p,\qquad(6)$$

where M is the mutual inductance, $I(0)$ is the transmission line current operator, given by Eq. (74) (see Appendix), at the qubit's position, $x = 0$.

The transmission line is considered to be driven by two fields. One is the probing field with the amplitude V_1^+ and the frequency ω close to the resonator characteristic frequency ω_r, as described in the Appendix. The amplitude of this field is assumed so small that its effect on the qubit can be neglected. (This is similar to the situation of coupling to the classical resonator considered in [35], where the small rf current was used to probe the resonator and also ac flux was applied to drive the qubit.) Another field describes driving the qubit with the amplitude ξ and the frequency ω_d. The Hamiltonian of this field, described by the periodic exchange of the photons between the resonator and the driving field, can be written as following:

$$H_{\mu w} = \xi\left(a^\dagger e^{-i\omega_d t} + a e^{i\omega_d t}\right).\qquad(7)$$

3. Energy levels and the spectroscopy of dressed states

Let us first diagonalize the qubit Hamiltonian, i.e., consider it in the eigenstate representation (see, e.g., Ref. 36). Then the qubit-resonator Hamiltonian can be written (without drive)

$$H'_{qb-r} = H'_0 + H'_{int},\qquad(8)$$

$$H'_0 = \frac{\hbar\omega_{qb}}{2}\sigma_z + \hbar\omega_r\left(a^\dagger a + \frac{1}{2}\right),\qquad(9)$$

$$H'_{int} = -\hbar g(a^\dagger + a)\left(\frac{\varepsilon}{\hbar\omega_{qb}}\sigma_z - \frac{\Delta}{\hbar\omega_{qb}}\sigma_x\right),\qquad(10)$$

where

$$\hbar\omega_{qb} = \sqrt{\Delta^2 + \varepsilon^2}\qquad(11)$$

is the bare qubit energy difference, $\sigma_{x,z}$ are Pauli matrices in the energy basis $\{|g\rangle, |e\rangle\}$ (so that $\sigma_z|g\rangle = -|g\rangle$). The bare system eigenstates are $|e/g, n\rangle = |e/g\rangle \otimes |n\rangle$ and eigenvalues

$$E_{e/g,n} = \pm\frac{\hbar\omega_{qb}}{2} + \hbar\omega_r\left(n + \frac{1}{2}\right).\qquad(12)$$

If the frequency ω_r is close to the gap frequency of the qubit ω_{qb} (for definitiveness we assume here $\omega_r > \omega_{qb}$) then for each n there are pairs of levels $|e, n\rangle$ and $|g, n+1\rangle$ which are close by the energy. Therefore, in order to find the modification of these levels by the interaction (10), we account only for the transitions between these two levels:

$$\langle g, n+1 | H'_{int} | e, n \rangle = \langle e, n | H'_{int} | g, n+1 \rangle = \hbar g_\varepsilon \sqrt{n+1}, \quad (13)$$

$$g_\varepsilon = g \frac{\Delta}{\hbar \omega_{qb}}. \quad (14)$$

(Note that away from the degeneracy point ($\varepsilon = 0$) the coupling strength is reduced by $\Delta / \hbar \omega_{qb}$ [21].) This leads to the new eigenvectors of the Hamiltonian H'_{qb-r} which can be expressed in terms of the eigenvectors of bare Hamiltonian H'_0 as following:

$$\begin{pmatrix} |-, n\rangle \\ |+, n\rangle \end{pmatrix} = \begin{pmatrix} \sin\eta & \cos\eta \\ -\cos\eta & \sin\eta \end{pmatrix} \begin{pmatrix} |g, n+1\rangle \\ |e, n\rangle \end{pmatrix}. \quad (15)$$

Then the solution of the eigenvalue problem is given by the following:

$$\tan 2\eta = \frac{2 g_\varepsilon \sqrt{n+1}}{\delta}, \quad (16)$$

$$E_{\pm, n} = \hbar \omega_r (n+1) \pm \frac{\hbar \Omega_n}{2}, \quad (17)$$

$$\Omega_n = \sqrt{4 g_\varepsilon^2 (n+1) + \delta^2}, \quad (18)$$

$$\delta = \omega_{qb} - \omega_r < 0. \quad (19)$$

The energy of the ground state, $|g, 0\rangle$, is given by

$$E_{gr} \equiv E_{g,0} = -\frac{\hbar \delta}{2}. \quad (20)$$

Here Ω_n defines the difference of energy levels: $E_{+, n} - E_{-, n} = \hbar \Omega_n$. In particular, the energy anticrossing takes place at $\delta = 0$, that is at $\hbar \omega_{qb}(\varepsilon^*) = \hbar \omega_r$, and it is given by

$$\Omega_n^{min} = \Omega_n(\varepsilon^*) = 2 g_{\varepsilon^*} \sqrt{n+1} = 2 g \frac{\Delta}{\hbar \omega_r} \sqrt{n+1}. \quad (21)$$

For example, in the inset in Fig. 2,*a* the energy anticrossing is shown for $n = 0$.

If the cavity is coupled to a weak drive field, one can achieve a regime when only few lower Fock states of the resonator are relevant (plotted with Eqs. (17) and (20) in Fig. 2,*a*). This allows the spectroscopy of the «dressed» energy levels: the transmission is resonantly increased when the drive photon energy $\hbar \omega_d$ matches the system energy difference from Eqs. (17) and (20) — shown with double arrows in Fig. 2,*a* for two possible frequencies. One can plot then the respective energy contour lines to de-
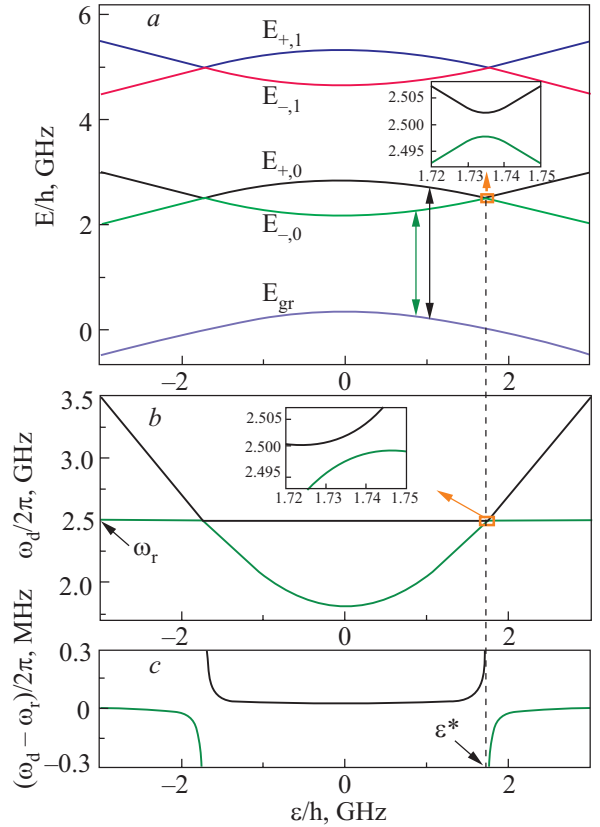

Fig. 2. (Color online) (*a*) Energy levels versus energy bias ε. Avoided level crossing is shown as a close-up in the inset. Parameters for this and the subsequent figures: $\Delta/h = 1.8$ GHz, $g/2\pi = 3$ MHz, $\omega_r/2\pi = 2.5$ GHz. (*b*) Contour lines of the energy difference versus bias ε and the driving frequency ω_d. Green (lower) line is for $\hbar \omega_d = E_{-,0} - E_{gr}$ and the black (upper) line is for $\hbar \omega_d = E_{+,0} - E_{gr}$. (*c*) Same as in (*b*) — in the very narrow vicinity of the resonator fundamental frequency ω_r.

scribe experimental results — see Figs. 2,*b,c*, which relate to the experimental Figs. 2 and 3 from Ref. 31. If the driving amplitude is increased, one should expect both multiphoton transitions as well as the involving qubit's upper levels, see Refs. 30, 37.

4. Hamiltonian of the system

4.1. Jaynes–Cummings Hamiltonian

Let us rewrite the interaction Hamiltonian, Eq. (10), by introducing the qubit lowering and raising operators

$$\sigma = \frac{1}{2}(\sigma_x - i\sigma_y) \text{ and } \sigma^\dagger = \frac{1}{2}(\sigma_x + i\sigma_y), \quad (22)$$

so that $\sigma^\dagger |g\rangle = |e\rangle$, $\sigma^\dagger |e\rangle = 0$, etc.; then we have

$$H'_{int} = \hbar g_\varepsilon (a^\dagger \sigma + a \sigma^\dagger) + \hbar g_\varepsilon (a\sigma + a^\dagger \sigma^\dagger) -$$

$$- \hbar g \frac{\varepsilon}{\hbar \omega_{qb}} (a^\dagger + a) \sigma_z. \quad (23)$$

The second and the third term in Eq. (23) can be neglected in the RWA since they do not conserve the number of photons in the system (this will also be justified in the next paragraph). The first term together with H_0' from Eq. (9) make the Jaynes–Cummings Hamiltonian:

$$H_{JC} = \frac{\hbar\omega_{qb}}{2}\sigma_z + \hbar\omega_r\left(a^\dagger a + \frac{1}{2}\right) + \hbar g_\varepsilon(a^\dagger\sigma + a\sigma^\dagger). \quad (24)$$

4.2. Interaction representation

Consider the Hamiltonian of interaction H_{int}' in the interaction representation. For this we note the following relations (see, e.g., [38]):

$$e^{ia^\dagger a\omega t}ae^{-ia^\dagger a\omega t} = ae^{-i\omega t}, \quad (25)$$

$$e^{i\frac{\omega}{2}t\sigma_z}\sigma e^{-i\frac{\omega}{2}t\sigma_z} = \sigma e^{-i\omega t}. \quad (26)$$

Then we obtain

$$H_{int}^I = e^{\frac{i}{\hbar}H_0't}H_{int}'e^{-\frac{i}{\hbar}H_0't} = \hbar g_\varepsilon\left(a\sigma^\dagger e^{i(\omega_{qb}-\omega_r)t} + \text{h.c.}\right) +$$

$$+\hbar g_\varepsilon\left(a\sigma e^{-i(\omega_{qb}+\omega_r)t} + \text{h.c.}\right) - \hbar g\frac{\varepsilon}{\hbar\omega_{qb}}\left(ae^{-i\omega_r t} + \text{h.c.}\right). \quad (27)$$

In the RWA, when $\omega_{qb} - \omega_r \ll \omega_{qb}$, the first term is slowly rotating, while the second and third terms are fast rotating ones. This justifies neglecting these terms in the RWA.

4.3. Rotating-wave approximation

Consider the Hamiltonian of the driven system in the RWA:

$$H_{RWA} = U\left(H_{qb-r}' + H_{\mu w}\right)U^\dagger + i\hbar\dot{U}U^\dagger. \quad (28)$$

For this we choose the transformation

$$U = \exp\left[i\omega_d t\left(a^\dagger a + \sigma_z/2\right)\right] \quad (29)$$

and obtain

$$H_{RWA} = \hbar\frac{\delta\omega_{qb}}{2}\sigma_z + \hbar\delta\omega_r a^\dagger a + \hbar g_\varepsilon(a\sigma^\dagger + a^\dagger\sigma) +$$

$$+\xi(a^\dagger + a), \quad (30)$$

$$\delta\omega_{qb} = \omega_{qb} - \omega_d, \quad (31)$$

$$\delta\omega_r = \omega_r - \omega_d. \quad (32)$$

4.4. With separate control microwave line

For the sake of generality, consider also the case when qubit is driven by the separate control line. Then instead of Eq. (7) we have

$$H_{\mu w}^{(2)} = -I_p\Phi_{ac}\cos\omega_d t \cdot \tau_z, \quad (32)$$

where Φ_{ac} is the amplitude of the driving flux. This expression in the qubit eigenstate representation gives the following:

$$H_{\mu w}^{(2)'} = -I_p\Phi_{ac}\frac{e^{i\omega_d t} + e^{-i\omega_d t}}{2}\left(\frac{\varepsilon}{\hbar\omega_{qb}}\sigma_z - \frac{\Delta}{\hbar\omega_{qb}}\sigma_x\right) \approx$$

$$\approx \xi_\varepsilon(e^{i\omega_d t}\sigma + e^{-i\omega_d t}\sigma^\dagger), \quad (33)$$

$$\xi_\varepsilon = \frac{1}{2}I_p\Phi_{ac}\frac{\Delta}{\hbar\omega_{qb}}. \quad (34)$$

Here we have left only slowly rotating terms (see discussion above). Note that the amplitude ξ_ε is dependent on the bias ε (see Eq. (11)). Then in the RWA after the transformation (29) we obtain the expression which differs from Eq. (30) by substituting the last term, $\xi(a^\dagger + a)$, with $\xi_\varepsilon(\sigma^\dagger + \sigma)$.

4.5. Dispersive regime

In the dispersive regime (that is far from resonance, where $\delta = 0$) the diagonalization of the Hamiltonian (24) in the second order in g/δ [38] gives

$$H = -\frac{1}{2}\left(\hbar\omega_{qb} + \frac{\hbar g_\varepsilon^2}{\delta}\right)\sigma_z + \left(\hbar\omega_r + \frac{\hbar g_\varepsilon^2}{\delta}\sigma_z\right)a^\dagger a. \quad (35)$$

This expression explicitly shows, first, how the qubit transition energy is shifted (normalized) by the coupling and, second, how the resonator energy $\hbar\omega_r$ is shifted by the qubit in different directions depending on the qubit state.

5. Solution of the master equation for the density matrix of the system

To describe the qubit-resonator dissipative dynamics we have to solve the master equation for the density matrix ρ:

$$\dot\rho = -\frac{i}{\hbar}[H,\rho] + \mathcal{L}[\rho]. \quad (36)$$

It includes the dynamic part and dissipative Lindblad term [39]

$$\mathcal{L}[\rho] = \frac{1}{2}\sum_{k=1}^{3}\left(2C_k\rho C_k^\dagger - C_k^\dagger C_k\rho - \rho C_k^\dagger C_k\right), \quad (37)$$

where

$$C_1 = \sqrt{\gamma_1}\sigma, \quad \gamma_1 = \frac{1}{T_1}, \quad (38)$$

$$C_2 = \sqrt{\frac{\gamma_\phi}{2}}\sigma_z, \quad \gamma_\phi = \frac{1}{T_\phi} = \frac{1}{T_2} - \frac{1}{2T_1},$$

$$C_3 = \sqrt{\varkappa}a.$$

Lindblad operator $\mathcal{L}$ presents dissipation in the resonator (photon decay) with the rate $\varkappa$, and the qubit decohe-

rence: the relaxation rate γ_1 and the dephasing rate γ_ϕ. We consider nondispersive regime (near the qubit-resonator resonance). Hamiltonian of the system H in the rotating wave approximation has the form of Eq. (30). Solution of the master equation determines the observable quantities, in particular, the expectation value of the photon field in the resonator

$$\langle a \rangle = \mathrm{Tr}(a\rho). \tag{39}$$

The Hilbert space of the composite system H_{QR} is the tensor product of qubit space H_Q and photon (resonator) space H_R: $H_{QR} = H_Q \otimes H_R$ with bases vectors $|e/g,n\rangle = |e/g\rangle \otimes |n\rangle$. Bases vectors $|g\rangle$ and $|e\rangle$

$$|g\rangle = \begin{bmatrix} 1 \\ 0 \end{bmatrix}, \quad |e\rangle = \begin{bmatrix} 0 \\ 1 \end{bmatrix} \tag{40}$$

are the eigenvectors of the operator σ_z. Fock vectors of the photon field $|n\rangle$ (the eigenvectors of photons number operator $a^\dagger a |n\rangle = n|n\rangle$) are vectors in infinite-dimensional space $N = \infty$:

$$|0\rangle = \begin{bmatrix} 1 \\ 0 \\ 0 \\ 0 \\ \vdots \end{bmatrix}, \quad |1\rangle = \begin{bmatrix} 0 \\ 1 \\ 0 \\ 0 \\ \vdots \end{bmatrix}, \quad |2\rangle = \begin{bmatrix} 0 \\ 0 \\ 1 \\ 0 \\ \vdots \end{bmatrix}, \quad \dots \; |n\rangle = \begin{bmatrix} 0 \\ 0 \\ \vdots \\ 1 \\ \vdots \end{bmatrix}. \tag{41}$$

In the basis $|e/g,n\rangle$ the matrix equation (36) is the infinite set of equations for infinite-dimensional matrix ρ_{ij}.

In the following we consider the case of $N = 2$, which allows the analytical solution, and in the case $N \gg 1$ we study the problem numerically.

5.1. Weak driving limit

To find the analytical solution we restrict the photon space to $N = 2$, supposing that mean photon number in resonator (created by the driving field with amplitude ξ) is much less than unity. The basis $|e/g,n\rangle$ in this case consists of 4 base vectors b_i:

$$b_1 = |g0\rangle, \; b_2 = |e0\rangle, \; b_3 = |g1\rangle, \; b_4 = |e1\rangle, \tag{42}$$

and the density matrix $\rho_{ij} = \langle b_i | \rho | b_j \rangle$ takes the form

$$\rho = \begin{pmatrix} \rho_{g0,g0} & \rho_{g0,e0} & \rho_{g0,g1} & \rho_{g0,e1} \\ \rho_{e0,g0} & \rho_{e0,e0} & \rho_{e0,g1} & \rho_{e0,e1} \\ \rho_{g1,g0} & \rho_{g1,g0} & \rho_{g1,g1} & \rho_{g1,e1} \\ \rho_{e1,g0} & \rho_{e1,e0} & \rho_{e1,g1} & \rho_{e1,e1} \end{pmatrix}. \tag{43}$$

In the steady state from Eq. (36) we have 16 linear equations for matrix elements ρ_{ij}. In the weak driving limit, leaving the terms up to the first order in the amplitude ξ, we obtain the density matrix ρ. Nonzero elements of matrix ρ_{ij} in the weak driving limit are

$$\rho_{g0,g0} = 1,$$

$$\rho_{g1,g0} = \rho_{g0,g1}^* = \frac{\xi(\delta\omega_{\mathrm{qb}} - i\gamma)}{g_\varepsilon^2 - (\delta\omega_r - i\varkappa/2)(\delta\omega_{\mathrm{qb}} - i\gamma)}, \tag{44}$$

$$\rho_{e0,g0} = \rho_{g0,e0}^* = \frac{\xi g_\varepsilon}{g_\varepsilon^2 - (\delta\omega_r - i\varkappa/2)(\delta\omega_{\mathrm{qb}} - i\gamma)},$$

where $\gamma = (\gamma_1/2) + \gamma_\phi$.

Putting (43) in (39) we obtain for the average value of the photon field in the resonator in the weak driving (WD) limit

$$\langle a \rangle_{WD} = \frac{\xi(\delta\omega_{\mathrm{qb}} - i\gamma)}{g_\varepsilon^2 - (\delta\omega_r - i\varkappa/2)(\delta\omega_{\mathrm{qb}} - i\gamma)}. \tag{45}$$

The transmission amplitude of the output driving signal $|t|$ is defined by the photon field in the resonator, Eq. (100) (see Appendix), and in accordance with (45) we obtain

$$|t|_{WD} = \left| \frac{\varkappa}{2} \mathrm{Im} \frac{\delta\omega_{\mathrm{qb}} - i\gamma}{g_\varepsilon^2 - (\delta\omega_r - i\varkappa/2)(\delta\omega_{\mathrm{qb}} - i\gamma)} \right|. \tag{46}$$

We have normalized $|t|$ on the value when the qubit is decoupled from the resonator, $g = 0$, and $\omega_d = \omega_r$.

The plot of the transmission amplitude $|t|_{WD}$, given by Eq. (46), is shown in Fig. 3 for $\omega_{\mathrm{qb}} = \omega_r$ and different values of the decaying rates $\varkappa$ and γ (given in units of the coupling constant g_ε). For small decaying rates $\varkappa$ and γ the transmission spectrum displays the Rabi-splitting peaks (solid curve), which are smeared with increasing of the decaying.

In Fig. 4 the density plot of the transmission amplitude as a function of the bias ε and the detuning $\omega_d - \omega_r$ is
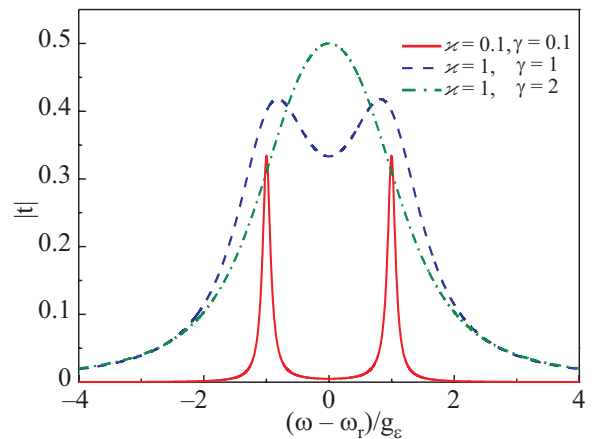

Fig. 3. (Color online) Normalized transmission amplitude $|t|$ as a function of the driving frequency detuning $\omega_d - \omega_r$ at $\varepsilon = \varepsilon^*$ (when $\omega_{\mathrm{qb}}(\varepsilon^*) = \omega_r$) for different values of the decaying rates $\varkappa$ and γ (given in the figure in units of g_ε), calculated with Eq. (46).
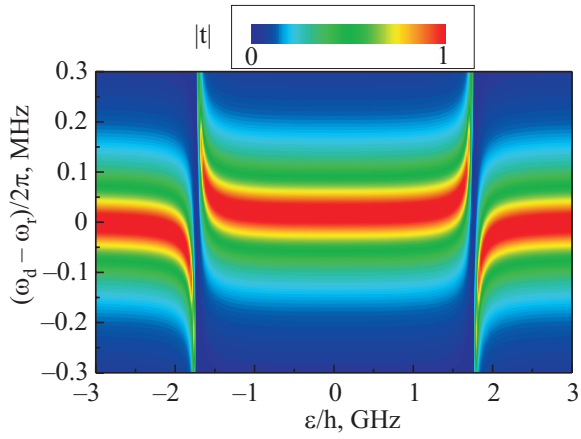
Fig. 4. (Color online) Normalized transmission amplitude $|t|$ as a function of the bias ε and the driving frequency detuning $\omega_d - \omega_r$, calculated with Eq. (46).

shown. The parameters here and below are taken for the comparison with the relevant experimental work [31]: $\Delta / h = 1.8$ GHz, $g / 2\pi = 3$ MHz, $\omega_r / 2\pi = 2.5$ GHz (the same as in Fig. 2) and also the loss rate of the resonator $\varkappa / 2\pi = 1.25 \cdot 10^{-4}$ GHz and the loss rate of the qubit $\gamma = g$. Note that we consider the intermediate coupling regime, when $g = \gamma \gg \varkappa$. The transmission amplitude is resonantly increased along the lines shown in Fig. 2,c as expected. The small vicinity of the resonator characteristic frequency, $\omega_d \in (\omega_r - g, \omega_r + g)$, allows to demonstrate the avoided crossing at $\varepsilon = \varepsilon^*$, as it was reported in Ref. 31.

For more detailed comparison and determining the not well known parameters (e.g., decay rate γ) it is needed to compare experimental and theoretical sets of cros-sections of surface $|t|$ versus ε and ω_d. In such way it is shown in Fig. 5 for $\omega_d = \omega_r$.
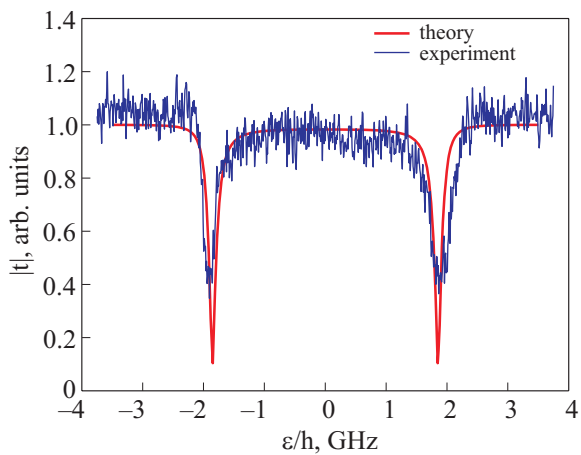

Fig. 5. (Color online) Normalized transmission amplitude $|t|$ as a function of the bias ε for $\omega_d = \omega_r$ calculated with Eq. (46) and obtained experimentally.

6. Numeral solution of the master equation for the density matrix. Beyond the weak driving regime

In the case of not small driving amplitudes, i.e., when the mean photon number $\langle a^\dagger a \rangle \gtrsim 1$, we have solved the equation for the density matrix ρ numerically. Results are presented in Fig. 6. The transmission amplitude $|t|$ in all cases is normalized on the maximal value; as above $\omega_{qb} = \omega_r$. In Fig. 6,a the transmission amplitude is shown for the case of small damping: $\varkappa / g_\varepsilon = 0.1$ and $\gamma / g_\varepsilon = 0.1$. At small value of the driving amplitude ξ the solid curve in Fig. 6,a coincides with the dependence $|t|_{WD} (\omega_d)$ (Fig. 3). With increasing of ξ each splitted Rabi peak is supersplitted (dashed curve) (see also in Ref. 40). With further increasing of the amplitude ξ, this supersplitting is smeared (dotted-dashed curve). Thus in the nonlinear regime we observe the qualitatively new features as compared to the weak driving limit.

When the decaying is rather large, such that in the weak-driving case, we do not have the Rabi splitting (dotted-dashed curve in Fig. 3), in the nonlinear response we do not have the qualitatively new features. It is shown in Fig. 6,b ($\varkappa / g_\varepsilon = 1$ and $\gamma / g_\varepsilon = 2$).
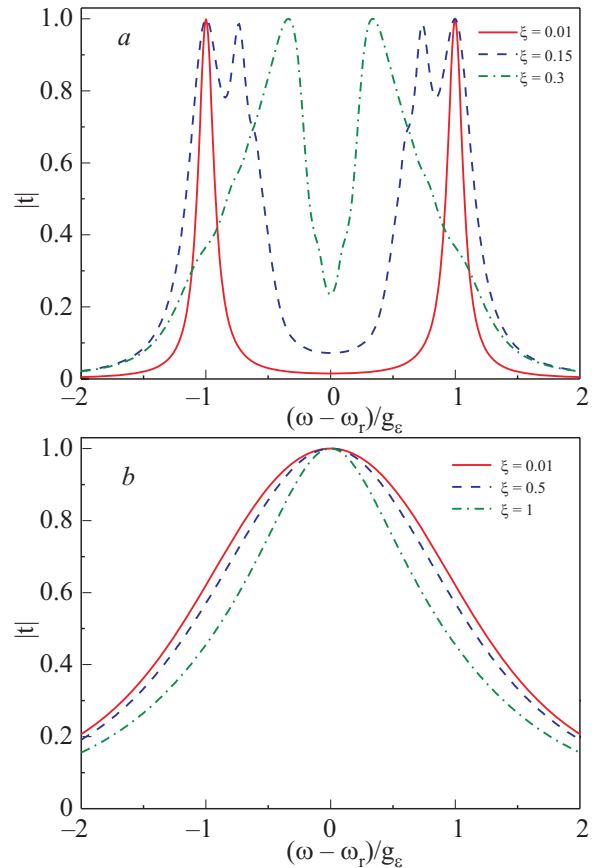

Fig. 6. (Color online) Normalized transmission amplitude $|t|$ as a function of the driving frequency detuning $\omega_d - \omega_r$ at $\varepsilon = \varepsilon^*$ (when $\omega_{qb}(\varepsilon^*) = \omega_r$) for (a) $\varkappa / g_\varepsilon = 0.1$, $\gamma / g_\varepsilon = 0.1$ and (b) $\varkappa / g_\varepsilon = 1$, $\gamma / g_\varepsilon = 2$, calculated by solving numerically the master equation for several values of ξ, given in units of g_ε.

We also calculated the average number of photons in the resonator, $n = \left\langle a^\dagger a \right\rangle$. For the parameters in Fig. 6 it depends on the frequency; the maximal values are the following: $n_{max} = 0.005$ for $\xi / g_\varepsilon = 0.01$, $n_{max} = 0.3$ for $\xi / g_\varepsilon = 0.15$, $n_{max} = 1.8$ for $\xi / g_\varepsilon = 0.3$.

7. Conclusions

We presented the detailed theory for the system of the flux qubit coupled inductively to the transmission line resonator. The transmission coefficient was calculated with the system's density matrix by solving the master equation within RWA.

The avoided crossing of the dressed energy levels was shown in the resonant case, where $\omega_d \approx \omega_{qb} \approx \omega_r$. This was demonstrated in the intermediate coupling regime, which describe the experimental results of Oelsner et al. [31]. We have shown that the dissipation smears the Rabi splitting. Moreover, we have demonstrated the supersplitting in the strong driving regime.

Appendix: Transmission line resonator

In this Appendix we consider the resonator formed by the transmission line interrupted by two capacitances C_0. The qubit we assume to be coupled inductively to the resonator at its center, see Fig. 1,*a*. We start by presenting the equations which describe the superconducting transmission line.

The transmission line

The transmission line can be modelled as an infinite alteration of the elementary circuits (e.g., [41]), as shown in Fig. 1,*b*. Here elementary inductance, capacitance and conductance are given by the values per unit length: $\Delta L = L\Delta x$, $\Delta C = C\Delta x$, $\Delta G = G\Delta x$.

Looking at the circuit in Fig. 1,*b*, we can write (neglecting the Ohmic losses) the following equations, by applying the Kirchhoff's laws for the voltage $V(x,t)$ and the current $I(x,t)$; in the limit $\Delta x \to 0$ they take the form

$$\frac{\partial V(x,t)}{\partial x} = -L\frac{\partial I(x,t)}{\partial t}, \tag{47}$$

$$\frac{\partial I(x,t)}{\partial x} = -GV(x,t) - C\frac{\partial V(x,t)}{\partial t}. \tag{48}$$

These equations can be rewritten for either $I(x,t)$ or $V(x,t)$ as following:

$$\frac{\partial^2 A}{\partial x^2} - \frac{1}{v^2}\frac{\partial^2 A}{\partial t^2} = \frac{\varkappa}{v^2}\frac{\partial A}{\partial t}, \quad A = \{I,V\}, \tag{49}$$

$$v = 1 / \sqrt{LC}, \tag{50}$$

$$\varkappa = G / C. \tag{51}$$

Here v has the meaning of the phase velocity and $\varkappa$ defines the loss in the transmission line.

Assuming $I(x,t) = I(x)e^{i\omega t}$ and $V(x,t) = V(x)e^{i\omega t}$, we obtain

$$\frac{dV(x)}{dx} = -i\omega LI(x), \tag{52}$$

$$\frac{dI(x)}{dx} = -(G + i\omega C)V(x). \tag{53}$$

Then equation for $A(x) = \{I(x),V(x)\}$ can be written as following:

$$\frac{d^2 A(x)}{dx^2} - \gamma^2 A(x) = 0, \tag{54}$$

$$\gamma = \sqrt{i\omega L(G + i\omega C)} \equiv \alpha + ik. \tag{55}$$

Solving equation for $V(x)$ and making use of Eq. (52), we obtain

$$V(x) = V_0^+ e^{-\gamma x} + V_0^- e^{\gamma x}, \tag{56}$$

$$I(x) = \frac{V_0^+}{Z_0}e^{-\gamma x} - \frac{V_0^-}{Z_0}e^{\gamma x}, \tag{57}$$

where

$$Z_0 = \frac{i\omega L}{\gamma} \equiv Z_1 + iZ_2. \tag{58}$$

$$Z_1 = \frac{\omega Lk}{\alpha^2 + k^2}, \quad Z_2 = \frac{\omega L\alpha}{\alpha^2 + k^2}. \tag{59}$$

When losses in the line are small ($G \ll \omega C$), we obtain

$$k \approx \omega\sqrt{LC} = \frac{\omega}{v}, \quad \alpha \approx \frac{G}{2}\sqrt{\frac{L}{C}} = \frac{\varkappa}{2v}, \tag{60}$$

$$Z_1 = \sqrt{\frac{L}{C}}, \quad Z_2 = \frac{\omega L\alpha}{k^2}. \tag{61}$$

Here the constants V_0^+ and V_0^- stand for the amplitudes of the right- and left-moving waves and Z_0 is the transmission line characteristic (wave) impedance.

Open transmission-line resonator

Consider the open transmission line of the length l. The quality factor of the resonator can be written as following [41]:

$$Q = \frac{k}{2\alpha} = \frac{\omega_r C}{G} = \frac{\omega_r}{\varkappa}. \tag{62}$$

This relation can be seen as another definition of $\varkappa$: $\varkappa = \omega_r / Q$. Now let us define normal modes of the resonator without dissipation ($\varkappa = 0$). Then assuming zero current through the boundaries at $x = \pm l / 2$ we obtain

$$I_j(x) = \frac{V_0^+}{Z_0}\left(e^{-ik_j x} - (-1)^j e^{ik_j x}\right), \tag{63}$$

$$V_j(x) = V_0^+\left(e^{-ik_j x} + (-1)^j e^{ik_j x}\right), \tag{64}$$

where $k_j l = j\pi$, $j = 1, 2, 3, ...$ In particular, for the fundamental mode $j = 1$ of the resonator we obtain

$$I_1(x) = \frac{2V_0^+}{Z_0}\cos k_1 x, \tag{65}$$

$$V_1(x) = -2iV_0^+ \sin k_1 x. \tag{66}$$

For the fundamental mode $j = 1$ of the $\lambda / 2$ resonator ($l = \lambda / 2$) we have $k_r \equiv k_1 = \pi / l$, $\omega_r \equiv \omega_1 = k_1 v = = 2\pi / (2\sqrt{L_r C_r})$, where $L_r = Ll$ and $C_r = Cl$ are the total inductance and capacitance of the resonator.

Let us expand the current in the resonator with the normal modes. We will choose the factor in the expansion having in view analogy with the harmonic oscillators (see below):

$$I(x,t) = \sum \sqrt{\frac{2m_j}{L_r}}\omega_j q_j(t)\cos k_j x. \tag{67}$$

Then for the voltage we obtain

$$V(x,t) = -L\int_0^x dx' \frac{\partial I(x',t)}{\partial t} = -\sum \sqrt{\frac{2m_j}{C_r}}\dot{q}_j(t)\sin k_j x. \tag{68}$$

Next, the Hamiltonian is introduced as the total energy of the resonator:

$$H_r = \int_{-l/2}^{l/2} dx\left(\frac{CV^2}{2} + \frac{LI^2}{2}\right) = \frac{1}{2}\sum\left(m_j \dot{q}_j^2 + m_j \omega_j^2 q_j^2\right), \tag{69}$$

which formally coincides with the Hamiltonian of the system of harmonic oscillators. This allows to quantize the system with the generalized coordinates q_j and conjugate momenta $p_j = m_j \dot{q}_j$. It is convenient also to introduce the annihilation/creation operators:

$$a_j(t) = \frac{m_j \omega_j q_j + ip_j}{\sqrt{2m_j \hbar \omega_j}}, \quad a_j^\dagger(t) = \frac{m_j \omega_j q_j - ip_j}{\sqrt{2m_j \hbar \omega_j}}. \tag{70}$$

In these terms, the current and voltage operators and the Hamiltonian take the following form:

$$\hat{I} = \sum \sqrt{\frac{\hbar \omega_j}{L_r}}(a_j + a_j^\dagger)\cos k_j x, \tag{71}$$

$$\hat{V} = i\sum \sqrt{\frac{\hbar \omega_j}{C_r}}(a_j - a_j^\dagger)\sin k_j x, \tag{72}$$

$$\hat{H}_r = \sum \hbar \omega_j\left(a_j^\dagger a_j + \frac{1}{2}\right). \tag{73}$$

We consider the frequency close to the fundamental mode frequency ω_r, so in what follows we disregard other modes. For the fundamental mode, with $k_1 = \pi / l$ and omitting the index $j = 1$, we obtain

$$\hat{I} = I_{r0}(a + a^\dagger)\cos\frac{\pi x}{l}, \quad I_{r0} = \sqrt{\frac{\hbar \omega_r}{L_r}}, \tag{74}$$

$$\hat{V} = iV_{r0}(a - a^\dagger)\sin\frac{\pi x}{l}, \quad V_{r0} = \sqrt{\frac{\hbar \omega_r}{C_r}}, \tag{75}$$

where I_{r0} and V_{r0} stand for the zero-point root mean square (rms) current and voltage, and the Hamiltonian is given by Eq. (4). In particular, it follows that at the boundaries, $x = \pm l / 2$, there is no current, and voltage equals to $\pm W$, where

$$W = iV_{r0}\left\langle a - a^\dagger \right\rangle = -2V_{r0}\text{Im}\langle a \rangle. \tag{76}$$

Transmittance of the resonator

Consider now the situation where the input signal is injected in the transmission-line resonator at $x = -l / 2$ through the capacitance C_0 and the output signal is detected after another capacitance C_0 at $x = l / 2$. We will obtain the system of equations for V_i^+ and V_i^-, which define the classical current and voltage in ith region, $i = 1, 2, 3$, respectively, for $x < -l / 2$, $x \in (-l / 2, l / 2)$, and $x > l / 2$:

$$V_i(x) = V_i^+ e^{-\gamma x} + V_i^- e^{\gamma x}, \tag{77}$$

$$I_i(x) = \frac{V_i^+}{Z_0}e^{-\gamma x} - \frac{V_i^-}{Z_0}e^{\gamma x}. \tag{78}$$

We assume the matched termination (with impedance equal to Z_0), then there is no left-moving wave in the third region, $V_3^- = 0$. The boundary conditions for currents and voltages at the points $x = \pm l / 2$ are the following:

$$I_1(-l / 2) = I_2(-l / 2), \tag{79}$$

$$I_2(l / 2) = I_3(l / 2), \tag{80}$$

$$V_2(-l/2) = V_1(-l/2) + I_2(-l/2)/i\omega C_0, \qquad (81)$$

$$V_3(l/2) = V_2(l/2) + I_3(l/2)/i\omega C_0. \qquad (82)$$

For the output signal we obtain $V_3^+ = V_1^+ t$, $I_3^+ = = V_3^+/Z_0 = V_1^+ t/Z_0$,

$$t = \frac{4\theta^2}{4\theta^2 + 4i\theta - 1 + e^{-2\gamma l}}, \qquad (83)$$

where $\theta = \omega C_0 Z_0$.

The phase shift of the output signal relative to the phase of the input signal is $\varphi - kl$, where φ is the phase of the quantity t, Eq. (83):

$$\tan\varphi = \frac{\text{Im}\, t}{\text{Re}\, t}. \qquad (84)$$

The transmittance of the resonator is the ratio of the output power at the point $x = +l/2$ to the input power at the point $x = -l/2$:

$$T = \frac{P_{\text{out}}}{P_{\text{in}}} = \frac{V_{\text{out}}(l/2)I_{\text{out}}^*(l/2) + V_{\text{out}}^*(l/2)I_{\text{out}}(l/2)}{V_{\text{in}}(-l/2)I_{\text{in}}^*(-l/2) + V_{\text{in}}^*(-l/2)I_{\text{in}}(-l/2)}, \qquad (85)$$

where $V_{\text{in}}(x) = V_1^+ e^{-\gamma x}$, $I_{\text{in}}(x) = I_1^+ e^{-\gamma x}/Z_0$, $V_{\text{out}}(x) = = V_3^+ e^{-\gamma x}$, $I_{\text{out}}(x) = I_3^+ e^{-\gamma x}/Z_0$.

Hence, for the transmittance we obtain

$$T = |t|^2\, e^{-2\alpha l}. \qquad (86)$$

It is important to note that the losses enter the quantity t due to θ:

$$\theta = \frac{C_0}{C}(k + i\alpha). $$

If the losses are small ($\alpha \ll k^2$) we can write the transmittance near the first resonance ($\omega_r = v\pi/l$) in the Lorenzian form:

$$T = \frac{16\theta_1^4\omega_r^2}{(2\pi)^2}\Bigg\{ \frac{\omega_r^2}{(2\pi)^2}(4\theta_1^2 + 2\alpha l)^2 + $$

$$+ \left[\frac{\omega_r}{2\pi}(4\theta_1 + 2\alpha l) - \delta\omega \right]^2 \Bigg\}^{-1}, \qquad (87)$$

where $\theta_1 = \omega_r C_0 Z_1$, $\delta\omega = \omega - \omega_r$.

From Eq. (87) we see that the main resonance is shifted both due to losses α and capacitance C_0. The width of Lorenzian (87) is given by

$$\Delta\omega = \frac{\omega_r}{\pi}(4\theta_1^2 + 2\alpha l) \qquad (88)$$

with the quality factor

$$Q = \frac{\omega_r}{\Delta\omega} = \frac{\pi}{4\theta_1^2 + 2\alpha l} \qquad (89)$$

and transmittance at resonance

$$T_r = \frac{1}{(1 + \alpha l/2\theta_1)^2}. \qquad (90)$$

The first term in (88) defines the photon decay rate $\varkappa$ due to leakage through the capacitances C_0:

$$\varkappa = \frac{4\omega_r \theta_1^2}{\pi} = \frac{4\omega_r^2 C_0^2 Z_1}{Cl}. \qquad (91)$$

This rate is consistent with its definition given in Ref. 31.

Below we estimate the photon decay rate $\varkappa$ for coplanar waveguide resonator with its parameter taken from [42]: $l = 23$ mm, $\omega_r/2\pi = 2.5$ GHz, $C_0 = 1$ fF, $Z_1 = 50$ Ohm. From these values we obtain $\theta_1 = 7.8 \cdot 10^{-4}$. The capacitance per unit length C is calculated from the expression for θ_1 at resonance: $\theta_1 = \pi C_0/lC$. For C we thus obtain $C = 1.74 \cdot 10^{-10}$ F/m. Finally, for photon decay rate $\varkappa$ we obtain from (91): $\varkappa/2\pi = 1.95$ kHz. This value is about two times less than the corresponding experimental values obtained in [42]. We assume this discrepancy is due to dielectric losses associated with the quantity G. This allows us to estimate α from $4\theta_1^2 \approx 2\alpha l$: $\alpha \approx 5.3 \cdot 10^{-5}$ m^{-1}. Therefore, for G we obtain $G = 2\alpha/Z_1 \approx 2.12$ Ohm$^{-1}\cdot$m^{-1}.

Transmittance in the dispersive regime

In the dispersive regime coupling to the qubit can be described as an additional inductance L_q at the position $x = 0$. Such a problem is described by adding two more equations for $x = 0$ to the system of equations (79)–(82) which follows from Eq. (47) by adding to the r.h.s. the following term:

$$-\delta(x)M\frac{\partial I_q}{\partial t} = -\delta(x)L_q\frac{\partial I(x,t)}{\partial t}, \qquad (92)$$

where

$$L_q = M^2\frac{\partial I_q}{\partial\Phi}. \qquad (93)$$

In the ground state we have [43,44]

$$L_q = \frac{4M^2 I_p^2 \Delta^2}{(\Delta^2 + \varepsilon^2)^{3/2}}. \qquad (94)$$

The solution of the system of equations for the transmission coefficient can be written as following:

$$t = \left[\frac{1}{4\theta^2}\left(e^{-2\gamma l} - (1 - i2\theta)^2 \right) + i\frac{L_q}{8\theta C_0 Z_0^2}\left(e^{-\gamma l} - 1 + i2\theta \right)^2 \right]^{-1}. \qquad (95)$$

Here the first term describes the transmission without qubit, at $L_q = 0$; see Eq. (83). It describes the resonant transmission (with $t = 1$) at

$$\frac{\omega - \omega_r}{\omega_r} = \frac{2\theta}{\pi}. \qquad (96)$$

At this frequency we find the expression for the transmission phase (84):

$$\tan \varphi = -\frac{1}{2\pi}\left(\frac{C_r}{C_0}\right)^2 \frac{L_q}{L_r}, \tag{97}$$

where we have assumed $C_r L_q / C_0 L_r \ll 1$.

In the ground state we obtain

$$\tan \varphi = -A\left[1+\left(\varepsilon / \Delta\right)^2\right]^{-3/2}, \tag{98}$$

$$A = \frac{2}{\pi}\left(\frac{C_r}{C_0}\right)^2 \frac{\hbar g^2}{\omega_r \Delta}. \tag{99}$$

Transmittance in the resonant regime

From the solution of the system of equations (79)–(82) we can express the solution for the transmission also in terms of the field in the resonator: $V_3^+ = i2\theta e^{\gamma l}V_2^-$; then after the quantization of the field in the resonator (see Eq. (76)) we arrive at the expression for $t = V_3^+ / V_1^+$:

$$t = 2\theta \frac{W}{V_1^+} = -\varkappa \frac{\operatorname{Im}\langle a\rangle}{2\xi}, \tag{100}$$

which relates the transmission coefficient t with the photon field $\langle a\rangle$. Here we have taken into account that in Eq. (7): $\xi = C_0 V_{r0}V_1^+ / 2$.

1. E. Il'ichev, A.Yu. Smirnov, M. Grajcar, A. Izmalkov, D. Born, N. Oukhanski, Th. Wagner, W. Krech, H.-G. Meyer, and A. Zagoskin, *Fiz. Nizk. Temp.* **30**, 823 (2004) [*Low Temp. Phys.* **30**, 620 (2004)].

2. J.Q. You and F. Nori, *Physics Today* **58**(11), 42 (2005).

3. G. Wendin and V.S. Shumeiko, *arXiv:cond-mat/0508729*; *Fiz. Nizk. Temp.* **33**, 957 (2007) [*Low Temp. Phys.* **33**, 724 (2007)].

4. A. Zagoskin and A. Blais, *Phys. Canada* **63**, 215 (2007).

5. Yu.A. Pashkin, T. Yamamoto, O. Astafiev, Y. Nakamura, D.V. Averin, and J.S. Tsai, *Nature* **421**, 823 (2003).

6. A. Izmalkov, M. Grajcar, E. Il'ichev, Th. Wagner, H.-G. Meyer, A.Yu. Smirnov, M.H.S. Amin, Alec Maassen van den Brink, and A.M. Zagoskin, *Phys. Rev. Lett.* **93**, 037003 (2004).

7. D. Vion, A. Aassime, A. Cottet, P. Joyez, H. Pothier, C. Urbina, D. Esteve, and M.H. Devoret, *Science* **296**, 886 (2002).

8. I. Chiorescu, Y. Nakamura, C.J.P.M. Harmans, and J.E. Mooij, *Science* **299**, 1869 (2003).

9. I. Chiorescu, P. Bertet, K. Semba, Y. Nakamura, C.J.P.M. Harmans, and J.E. Mooij, *Nature* **431**, 160 (2004).

10. E. Il'ichev, N. Oukhanski, A. Izmalkov, Th. Wagner, M. Grajcar, H.-G. Meyer, A.Yu. Smirnov, Alec Maassen van den Brink, M.H.S. Amin, and A.M. Zagoskin, *Phys. Rev. Lett.* **91**, 097906 (2003).

11. J. Johansson, S. Saito, T. Meno, H. Nakano, M. Ueda, K. Semba, and H. Takayanagi, *Phys. Rev. Lett.* **96**, 127006 (2006).

12. A.N. Omelyanchouk, S. Savel'ev, A.M. Zagoskin, E. Il'ichev, and F. Nori, *Phys. Rev.* **B80**, 212503 (2009).

13. Y. Nakamura, Yu.A. Pashkin, T. Yamamoto, and J.S. Tsai, *Phys. Rev. Lett.* **88**, 047901 (2002).

14. D. Vion, A. Aassime, A. Cottet, P. Joyez, H. Pothier, C. Urbina, D. Esteve, and M.H. Devoret, *Fortschr. Phys.* **51**, 462 (2003).

15. A. Izmalkov, M. Grajcar, E. Il'ichev, N. Oukhanski, Th. Wagner, H.-G. Meyer, W. Krech, M.H.S. Amin, Alec Maassen van den Brink, and A.M. Zagoskin, *Europhys. Lett.* **65**, 844 (2004).

16. W.D. Oliver, Ya. Yu, J.C. Lee, K.K. Berggren, L.S. Levitov, and T.P. Orlando, *Science* **310**, 1653 (2005).

17. M. Sillanpää, T. Lehtinen, A. Paila, Yu. Makhlin, and P. Hakonen, *Phys. Rev. Lett.* **96**, 187002 (2006).

18. S.N. Shevchenko, S. Ashhab, and F. Nori, *Phys. Rep.* **492**, 1 (2010).

19. G. Sun, X. Wen, B. Mao, J. Chen, Y. Yu, P. Wu, and S. Han, *Nat. Commun.* **1**, 51 (2010).

20. R.J. Schoelkopf and S.M. Girvin, *Nature* **451**, 664 (2008).

21. A. Blais, R.-S. Huang, A. Wallraff, S.M. Girvin, and R.J. Schoelkopf, *Phys. Rev.* **A69**, 062320 (2004).

22. Y.X. Liu, C.P. Sun, and F. Nori, *Phys. Rev.* **A74**, 052321 (2006).

23. Y.-L. Chen, Y.-F. Xiao, X. Zhou, Xu-Bo Zou, Z.-W. Zhou, and G.-C. Guo, *J. Phys. B: At. Mol. Opt. Phys.* **41**, 175503 (2008).

24. J. Bourassa, J.M. Gambetta, A.A. Abdumalikov, Jr., O. Astafiev, Y. Nakamura, and A. Blais, *Phys. Rev.* **A80**, 032109 (2009).

25. S. Ashhab and F. Nori, *Phys. Rev.* **A81**, 042311 (2010).

26. A. Wallraff, D.I. Schuster, A. Blais, L. Frunzio, R.-S. Huang, J. Majer, S. Kumar, S.M. Girvin, and R.J. Schoelkopf, *Nature* **431**, 162 (2004).

27. D.I. Schuster, A. Wallraff, A. Blais, L. Frunzio, R.-S. Huang, J. Majer, S.M. Girvin, and R.J. Schoelkopf, *Phys. Rev. Lett.* **94**, 123602 (2005).

28. D.I. Schuster, *Circuit Quantum Electrodynamics*, PhD thesis, Yale University (2007).

29. T. Lindström, C.H. Webster, J.E. Healey, M.S. Colclough, C.M. Muirhead, and A.Y. Tzalenchuk, *Supercond. Sci. Technol.* **20**, 814 (2007).

30. A.A. Abdumalikov, Jr., O. Astafiev, Y. Nakamura, Yu.A. Pashkin, and J.S. Tsai, *Phys. Rev.* **B78**, 180502(R) (2008).

31. G. Oelsner, S.H.W. van der Ploeg, P. Macha, U. Hübner, D. Born, S. Anders, E. Il'ichev, H.-G. Meyer, M. Grajcar, S. Wünsch, M. Siegel, A.N. Omelyanchouk, and O. Astafiev, *Phys. Rev.* **B81**, 172505 (2010).

32. T.P. Orlando, J.E. Mooij, L. Tian, C.H. van der Wal, L.S. Levitov, S. Lloyd, and J.J. Mazo, *Phys. Rev.* **B60**, 15399 (1999).

33. O. Astafiev, A.M. Zagoskin, A.A. Abdumalikov, Jr., Yu.A. Pashkin, T. Yamamoto, K. Inomata, Y. Nakamura, and J.S. Tsai, *Science* **327**, 840 (2010).

34. L. Zhou, Z.R. Gong, Y.X. Liu, C.P. Sun, and F. Nori, *Phys. Rev. Lett.* **101**, 100501 (2008).

35. S.N. Shevchenko, S.H.W. van der Ploeg, M. Grajcar, E. Il'ichev, A.N. Omelyanchouk, and H.-G. Meyer, *Phys. Rev.* **B78**, 174527 (2008).

36. Ya.S. Greenberg, *Phys. Rev.* **B76**, 104520 (2007).

37. J.M. Fink, M. Göppl, M. Baur, R. Bianchetti, P.J. Leek, A. Blais, and A. Wallraff, *Nature* **454**, 315 (2008).

38. W.P. Schleich, *Quantum Optics in Phase Space*, Wiley-VCH, Berlin (2001).

39. M.O. Scully and M.S. Zubairy, *Quantum Optics*, Cambridge, Cambridge University Press (1997).

40. L.S. Bishop, J.M. Chow, J. Koch, A.A. Houck, M.H. Devoret, E. Thuneberg, S.M. Girvin, and R.J. Schoelkopf, *Nature Phys.* **5**, 105 (2009).

41. D.M. Pozar, *Microwave Engineering*, Wiley, New York, 3rd ed. (1990).

42. P. Macha, S.H.W. van der Ploeg, G. Oelsner, E. Il'ichev, H.-G. Meyer, S. Wünsch, and M. Siegel, *Appl. Phys. Lett.* **96**, 062503 (2010).

43. Ya.S. Greenberg, A. Izmalkov, M. Grajcar, E. Il'ichev, W. Krech, H.-G. Meyer, M.H.S. Amin, and A. Maassen van den Brink, *Phys. Rev.* **B66**, 214525 (2002).

44. M. Grajcar, A. Izmalkov, E. Il'ichev, Th. Wagner, N. Oukhanski, U. Hübner, T. May, I. Zhilyaev, H.E. Hoenig, Ya.S. Greenberg, V.I. Shnyrkov, D. Born, W. Krech, H.-G. Meyer, Alec Maassen van den Brink, and M.H.S. Amin, *Phys. Rev.* **B69**, 060501(R) (2004).